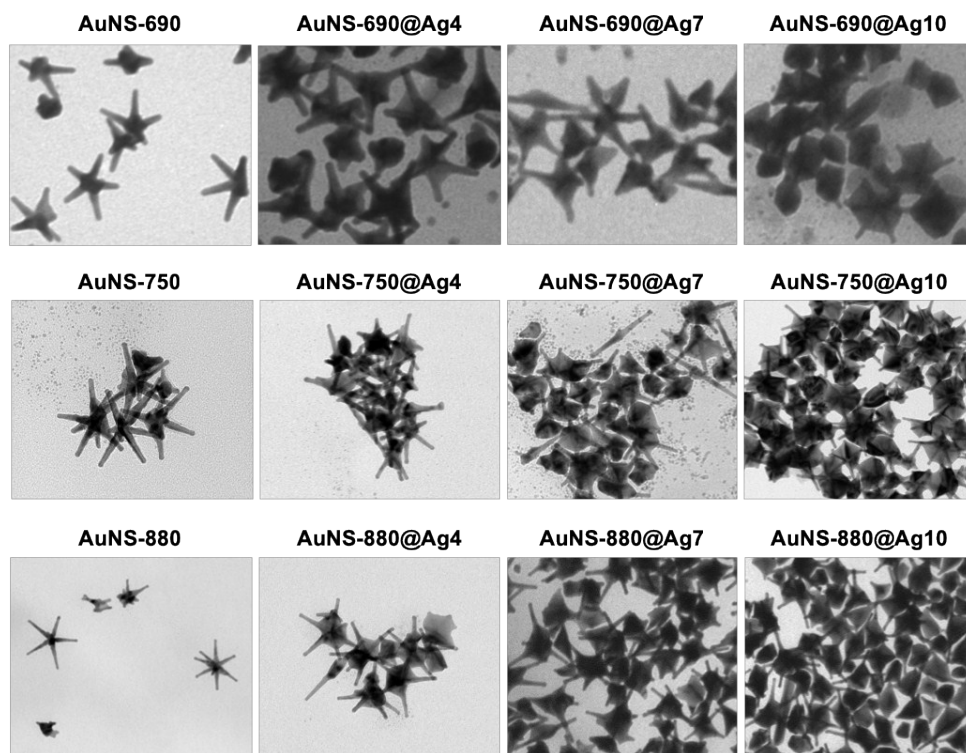# Supporting Information

Fig. S1. The TEM images of AuNS@Ag with different branch lengths which are named according to their intermediate absorption peaks as AuNS-690, AuNS-750 and AuNS-880, and different Ag shell thickness represented by the volume of $AgNO_3$ (0.1 M) added to the reaction mixture. AuNS@Ag4, AuNS@Ag7 and AuNS@Ag10 are AuNS@Ag with the addition of 4, 7 and 10 μL of $AgNO_3$ (0.1 M).
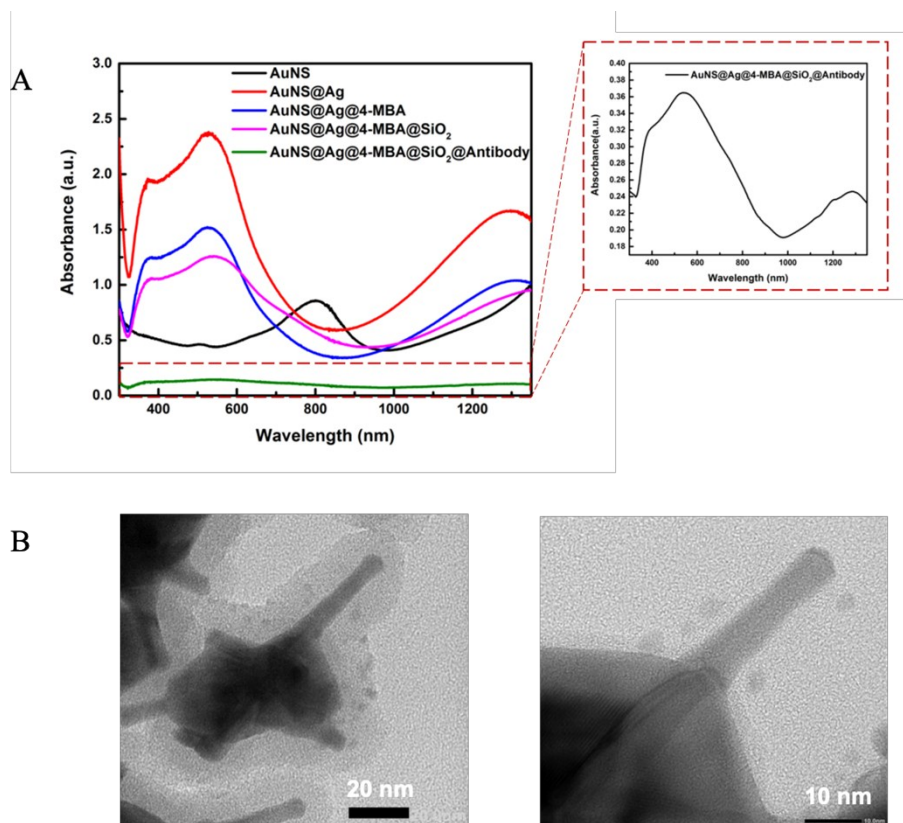
Fig. S2. (A) The absorption spectra of gold nanostar (AuNS), silver coated AuNS (AuNS@Ag) silica coated AuNS@Ag (AuNS@Ag@SiO$_2$), and anti-AFP antibody conjugated AuNS@Ag@SiO$_2$ (AuNS@Ag@SiO$_2$@Antibody); (B) TEM images of AuNS@Ag@SiO$_2$@Antibody, and the black dots surrounding the SiO$_2$ shell should be the conjugated antibodies.
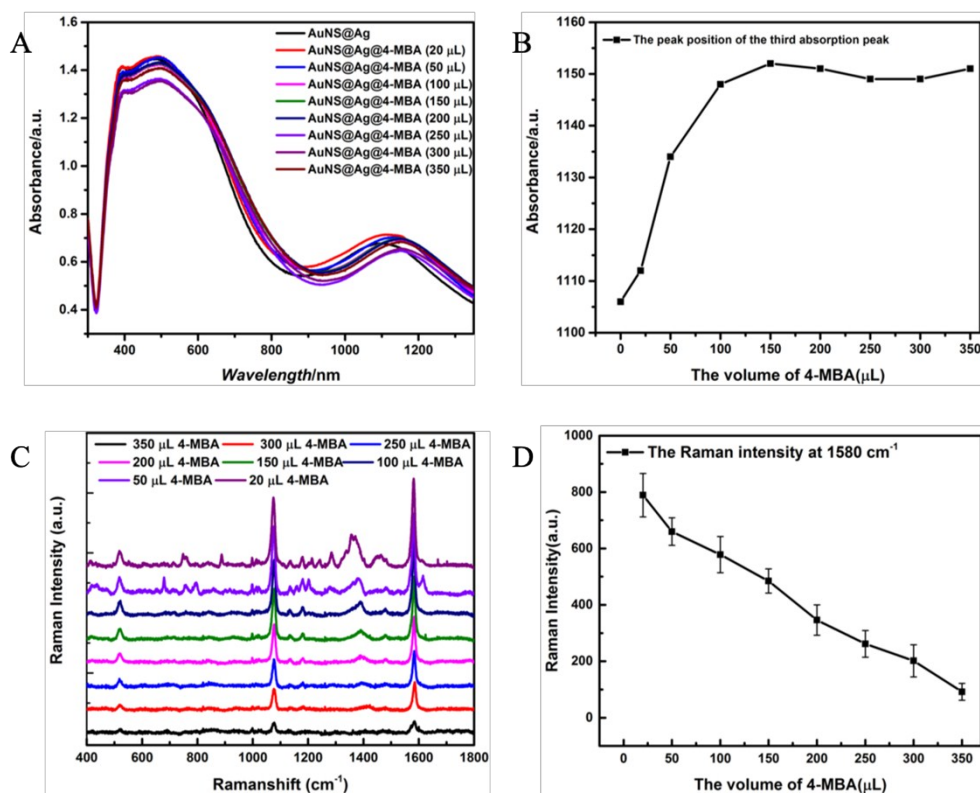
Fig. S3. (A) absorption spectra and (B) intensity of the third absorption peak of AuNS@Ag with the addition of different volume of 4-MBA (10^{-4} M) ranging from 20 to 350 µL; (C) the Raman spectra of 4-MBA and (D) the Raman intensity of 4-MBA at 1580 cm^{-1} with AuNS@Ag@4-MBA as substrate that were prepared with the addition of different volume of 4-MBA (10^{-4} M) ranging from 20 to 350 µL.
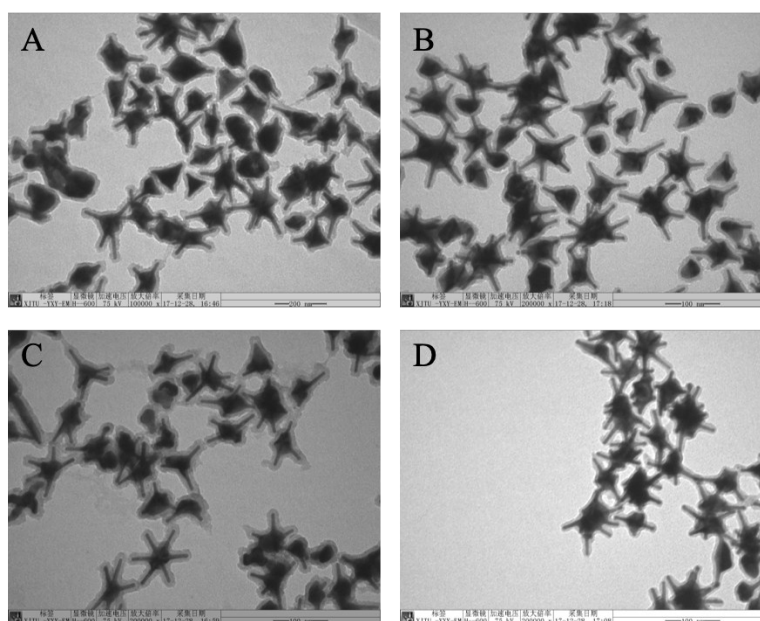

Fig. S4. TEM images of AuNS@Ag@SiO$_2$ of the same AuNS, the same Ag and SiO2 shell thicknesses prepared with different concentrations of SH-PEG-OH ranging from 10 to 40 µg/mL as stabilizer during the Stöber reactions.
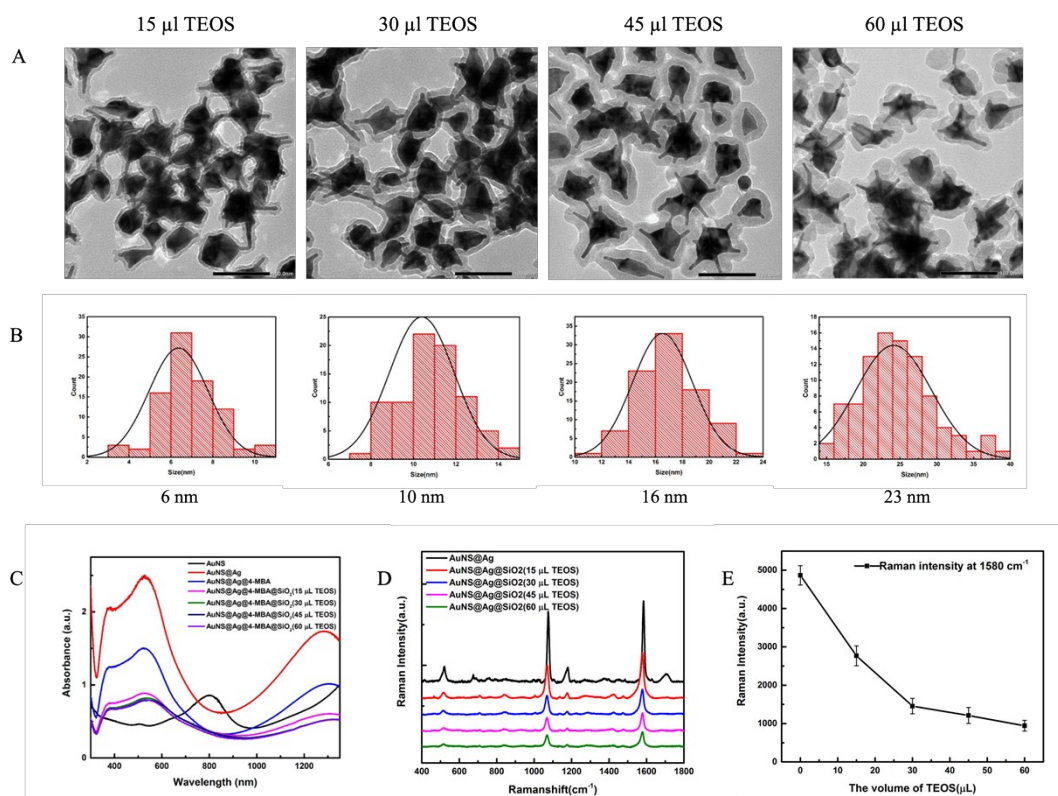
Fig. S5. (A) TEM images, (B) size distribution and (C) absorption spectra of AuNS@Ag@SiO$_2$ with SiO$_2$ shell thicknesses ranging from 6 nm to 23 nm synthesized by adding different volumes of tetraethyl orthosilicate (TEOS); (C) Raman spectra of 4-MBA and (E) the characteristic peak at 1580 cm^{-1} when AuNS@Ag and AuNS@Ag@SiO$_2$ with different SiO$_2$ shell thicknesses were used as SERS substrate.

AuNS@Ag@SiO$_2$ with SiO$_2$ thicknesses of approximately 6 nm, 20 nm, 16 nm, and 23 nm were synthesized by adding 15 µl, 30 µl, 45 µl, 60 µl volumes of TEOS, respectively. The TEM images shows that the silica is uniformly coated on the surface of the bimetallic nanoparticle and the thickness increases with the increase of TEOS volume (Fig. S5(A)). Compared to bare AuNS@Ag, silica coating results in a slight red-shift of the absorption spectra due to the presence of the dielectric layer which increases the refractive index around the metal nanostructure. As the thickness of this layer increases, the LSPR further shifted to longer wavelengths as shown in Fig. S5 (C). The Raman spectra of 4-MBA on AuNS@Ag@SiO$_2$ with different SiO$_2$ thicknesses and the corresponding SERS intensity of the characteristic peak at 1580 cm^{-1} are shown in Fig. S5 (D) and (E). It can be observed that the SERS intensity decreases significantly with the increase of silica shell thickness. The maximum SERS activity occurs at the smallest SiO$_2$ shell thickness which is 6 nm. Silica coating thinner than this value could not provide the bimetallic nanoparticles with sufficient colloidal stability and as a result aggregation occurred.

Table S1 Lengths of spikes of AuNS-880@Ag before and after silver coating with the addition of 4, 7 and 10 μL of AgNO$_3$

Volumes of AgNO$_3$ added for synthesizing AuNS-880@Ag	Length of Au branches before Ag coating	Length of Au branches after Ag coating
4 μL	46 nm	31.38 nm
7 μL	46 nm	28.52 nm
10 μL	46 nm	23.73 nm

Table S2 Lengths of the spikes and silver shell thicknesses of AuNS@Ag of different branch lengths and the maximum SERS activities

Name of AuNS@Ag with the maximum SERS activity	Lengths of Au branches before Ag coating	Lengths of Au branches after Ag coating	Silver shell thickness
AuNS-690@Ag7	30 nm	15.2 nm	14.4 nm
AuNS-750@Ag8	37 nm	17.4 nm	22.0 nm
AuNS-880@Ag11	46 nm	28.7 nm	28.5 nm